ELSEVIER

### Contents lists available at ScienceDirect

# **Food Chemistry**

journal homepage: www.elsevier.com/locate/foodchem





# Oil soluble iron: Curcumin derivatives and their complex

Amin Zarei<sup>1</sup>, Leila Khazdooz<sup>1</sup>, Anahita Khojastegi, Ataf Ali Altaf, Alireza Abbaspourrad<sup>3</sup>

Department of Food Science, College of Agriculture & Life Sciences, Cornell University, Stocking Hall, Ithaca, NY 14853, United States

ARTICLE INFO

Keywords:
Curcumin dibutanoate
Digestible ligand
Oil soluble ligand
Fe(CUDB)<sub>2</sub>
Oil-soluble iron (II) complex

### ABSTRACT

Curcumin dibutanoate (CUDB) is a new oil soluble bidentate ligand which shows higher stability against heat and oxidation compared to curcumin. The oil solubility of this ligand increased an order of magnitude over curcumin. This biomolecule showed high digestibility in a simulated intestinal trial and was hydrolyzed in the presence of porcine pancreatin releasing  $\sim 91\%$  of the curcumin. When curcumin dibutanoate was complexed with Fe<sup>2+</sup>, Fe (CUDB)<sub>2</sub> was formed as a new iron (II) complex. Due to the high hydrophobicity of the curcumin dibutanoate ligand, the solubility of Fe(CUDB)<sub>2</sub> was found to be 2.8 mg/mL in canola oil. The steric hindrance afforded by the CUDB ligand, coupled with its hydrophobicity stabilized the iron (II) oxidation state within the complex compared to FeSO<sub>4</sub>·7H<sub>2</sub>O as measured by 2,2-diphenyl-1-picrylhydrazyl (DPPH) radical. Fe(CUDB)<sub>2</sub> has potential to be a new form of oil-soluble iron supplement which co-delivers iron (II) and curcumin.

### 1. Introduction

Iron is an essential micronutrient that plays many vital roles within important biological processes (Abbaspour et al., 2014). Iron deficiency is a worldwide public health issue with an estimated 30% of the world's population having diets considered iron deficient (Lorinczova et al., 2021). In children, iron deficiency retards growth, impacts metabolism, and leads to potential cognitive impairment (Lopez et al., 2016). Iron deficiency in adults endangers both physical and cognitive performance and is often accompanied by fatigue, depression, and poor quality of life (Haas & Brownlie IV, 2001; Jáuregui-Lobera, 2014). Iron deficiency can be attributed to insufficient iron consumption, coupled with the intake of dietary iron inhibitors like polyphenols which lead to a notable decrease in iron absorption (Tuntipopipat et al., 2009). Oral iron supplementation with high doses of FeSO<sub>4</sub> can be a useful and effective method to decrease iron deficiency; however, ingestion of FeSO<sub>4</sub> is often accompanied by negative gastrointestinal side effects such as diarrhea, constipation, nausea, and epigastric discomfort (Lopez et al., 2016; Lorinczova et al., 2021). Too much iron is also problematic, especially in the gastrointestinal tract where it can facilitate the formation of destructive reactive oxygen species (ROS) which can damage the gastrointestinal mucosa and increase inflammation (Wessling-Resnick, 2017). Antioxidants can be used to deactivate the ROS formed in the gastrointestinal tract (Assunção et al., 2010).

Curcumin (1,7-bis(4-hydroxy-3-methoxyphenyl)-1,6-heptadiene-

Recently, we have shown that esterification of unstable natural products like nicotinamide riboside and catechin increases their stability and their solubility in oils (Kolba et al., 2022a, 2022b; Zarei et al.,

<sup>3,5-</sup>dione) is considered one of the best natural antioxidants (Wei et al., 2006). Classified as a non-flavonoid polyphenolic compound curcumin acts as an iron absorption inhibitor by decreasing the non-heme iron bioavailability (Tuntipopipat et al., 2009). Although curcumin inhibits iron uptake by complexing iron, it also stimulates iron absorption by decreasing the expression of hepcidin, the hormone responsible for iron regulation (Milman, 2020). Recent studies have shown that the use of curcumin along with iron supplements does not decrease iron absorption in healthy adults (Lorinczova et al., 2021). Co-administration of curcumin and FeSO<sub>4</sub> has been shown to increase the brain-derived neurotrophic factor in healthy adults, maintaining the normal neuronal function, and improving cognitive function (Tiekou Lorinczova et al., 2020). In addition to its antioxidant activity, curcumin also exhibits a variety of valuable physiological and pharmaceutical properties (Jurenka, 2009; Liu et al., 2016; Salem et al., 2014; Srivivasan et al., 2003). Unfortunately, curcumin has shown low bioavailability due to its insolubility in water, tendency toward auto-oxidation and ease of degradation (Salem et al., 2014; Schneider et al., 2015; Stohs et al., 2020). While researchers have found that consuming curcumin with a meal rich in fats increases its absorption (Stohs et al., 2020), the oil solubility of this compound is not sufficient to use as an additive in common oils like canola and olive oils.

<sup>\*</sup> Corresponding author.

E-mail address: Alireza@cornell.edu (A. Abbaspourrad).

<sup>&</sup>lt;sup>1</sup> These authors contributed equally to this work.

2021). The results of *in vitro* experiments reveal that these ester functionalities can be enzymatically hydrolyzed in simulated intestinal fluid to release the primary natural product (Zarei et al., 2021).

In this work, curcumin diacetate, curcumin dibutanoate, and curcumin dioctanoate were synthesized by the reaction between curcumin and the corresponding anhydrides in the presence of a catalytic amount of 4-dimethylamino pyridine (DMAP) (Scheme 1). Among these ester derivatives of curcumin, curcumin dibutanoate (CUDB), showed remarkably increased solubility in food grade oils. In addition, in vitro, CUDB was highly digestible and released curcumin (91%) in the presence of porcine pancreatin in a simulated intestinal trial. Because curcumin has also been shown to make metal-curcumin complexes that show enhanced pharmacological and therapeutic activities (Bicer et al., 2018; Prasad et al., 2021; Rainey et al., 2019), we investigated the ability of this curcumin ester derivative to chelate iron. We used CUDB and iron (II) sulfate to synthesize a new oil soluble iron (II) complex. Finally, we studied the antioxidant activity of these compounds in the presence of 2,2-diphenyl-1-picrylhydrazyl (DPPH) radical. Due to the presence of Fe<sup>2+</sup>, Fe(CUDB)<sub>2</sub> showed better results for radical scavenging activity in comparison to uncomplexed curcumin dibutanoate.

### 2. Materials and methods

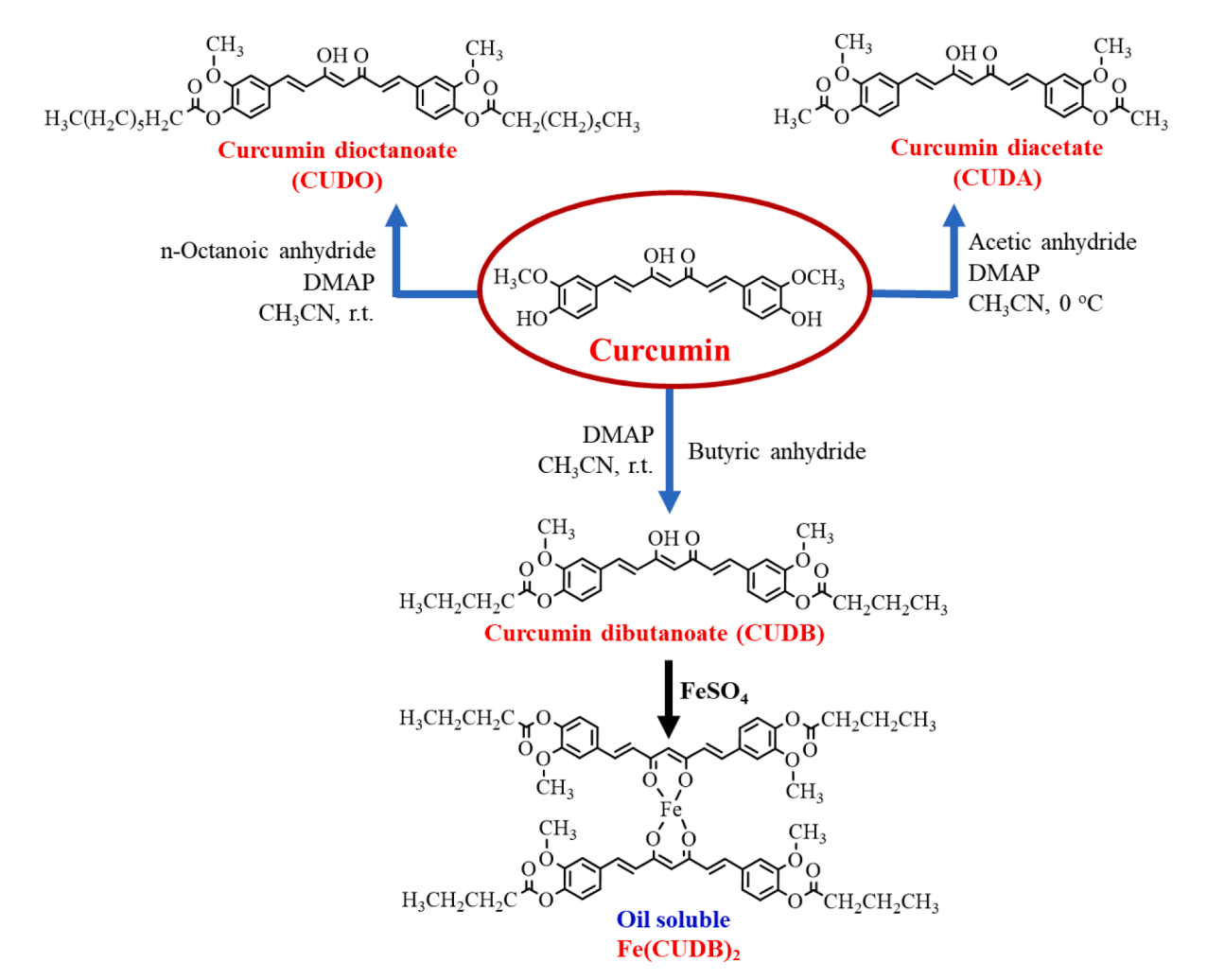
### 2.1. Materials

Acetic anhydride (99%), butyric anhydride (98%), 2,2-diphenyl-1-picrylhydrazyl (DPPH), and 4-dimethylamino pyridine (99%) were

purchased from Sigma-Aldrich (St. Louis, MO, USA). Curcumin (97%) and *n*-octanoic anhydride (95%) were purchased from the TCI Chemicals (Montgomeryville, PA, USA). Iron (II) sulfate heptahydrate (99%) was purchased from Sigma-Aldrich (St. Louis, MO, USA). Silica gel (P60, 40–63 µm, 60 Å) was purchased from SiliCycle, and Silica Gel 60 F254 Coated Aluminum-Backed TLC Plates were purchased from EMD Millipore (Billerica, MA, USA). Bile extract porcine (B8631) and pancreatin from porcine pancreas (P7545, 8 USP) were purchased from Sigma-Aldrich (St. Louis, MO, USA).

#### 2.2. Characterization

A 500 MHz NMR (Bruker AVANCE) spectrometer was used for  $^{1}$ H NMR (500 MHz) and  $^{13}$ C NMR (125 MHz) spectra. The chemical shifts were reported in δ (ppm) and coupling constants (J) were measured in Hz. Spin multiplicities were described as singlet (s), doublet (d), triplet (t), quartet (q), sextet (sext), and multiplet (m). Fourier transform infrared spectra (ATR-FTIR) were recorded on a Shimadzu IRAffinity-1S spectrophotometer. UV–vis was recorded on a Shimadzu UV-2600 spectrophotometer. EPR spectroscopy results was reported by a Bruker ELEXSYS X-band CW at 100 K. Scanning Electron Microscopy (SEM) was recorded using a Zeiss Gemini 500 Field Emission Scanning Electron Microscope. Thermogravimetric analysis (TGA) was run on a TA Instruments 5500 with platinum sample pans under an atmosphere of nitrogen and a heating rate of 10 °C min $^{-1}$ . X-ray diffraction (XRD) data were reported by a Bruker D8 Advance ECO powder diffractometer and Cu K-α radiation at  $\lambda = 1.54056$  Å, 40 kV, and 25 mA. X-ray



Scheme 1. Functionalization of curcumin to their corresponding ester derivatives and synthesis of Fe(CUDB)<sub>2</sub> as a new oil soluble iron (II) complex.

Photoelectron Spectroscopy (XPS) was performed using a Scienta Omicron ESCA 2SR with operating pressure ca.  $1 \times 10^{-9}$  Torr using a pass energy of 200 eV for wide/survey scans. For LC-MS analysis, we used an LC (Agilent 1100 series) coupled with a mass spectrometer. Reversephase chromatography was used with a Phenomenex Luna Omega (Phenomenex) LC column with the following specifications:  $100 \times 4.6$ mm, 3 µm, Luna C18(2), 100 Å pore size with a flow rate of 0.6 mL  $\mathrm{min}^{-1}$ . All samples were filtered by a 13 mm Nylon syringe filter with a  $0.22~\mu m$  pore size before measurement before injection. For the detection of curcumin dibutanoate, curcumin dioctanoate, and Fe(CUDB)2, the LC column was eluted with 85% DI water containing 0.1% formic acid, and 15% acetonitrile. For the detection of curcumin, the LC column was eluted with 15% DI water containing 0.1% formic acid, and 85%acetonitrile containing 0.1% formic acid. The injection volume was 10 μL for each sample. The mass spectrometer (Finnigan LTQ mass spectrometer) was equipped with an electrospray interface (ESI) set in positive electrospray ionization mode. The optimized parameters were a sheath gas flow rate at 50 arbitrary units, spray voltage set at 4.00 kV, capillary temperature at 350 °C, the capillary voltage at 41.0 V, and tube lens set at 125.0 V.

#### 2.3. Synthesis of curcumin diacetate

To a round bottom flask fitted with a magnetic stir bar, septa, and nitrogen inlet, 300 mg (0.815 mmol) of curcumin, 25 mg (0.20 mmol) of 4-dimethylamino pyridine, and 8 mL of acetonitrile were added. The flask was placed in an ice bath at 0 °C and 0.50 mL (5.3 mmol) of acetic anhydride was dropwise added to the reaction mixture and stirred for 1 h under nitrogen. The progress of the reaction was followed by thin-layer chromatography (TLC). After completing the reaction, 40 mL of ethyl acetate was added to the reaction mixture and the organic phase was washed with (4  $\times$  20 mL) of HCl (2 M). After that, the organic phase was washed with (3  $\times$  20 mL) of NaHCO3 (0.4 M). Then, the organic solvent was dried with anhydrous sodium sulfate and evaporated by a rotary evaporator. Finally, the crude product was washed with hexanes to obtain the pure product as a yellow solid in 82 % yield (300 mg). Characterization matches previous synthesis (Basile et al., 2009) (Figures S1-S3).

# 2.4. Synthesis of curcumin dioctanoate

To a round bottom flask with a magnetic stir bar, septa, and nitrogen inlet, 300 mg (0.815 mmol) of curcumin, 1.6 mL (5.1 mmol) of octanoic anhydride, 25 mg (0.2 mmol) of 4-dimethylamino pyridine, and 9 mL of acetonitrile were added. The reaction mixture was stirred at room temperature overnight under a nitrogen blanket. The progress of the reaction was followed by thin-layer chromatography (TLC). After completing the reaction, 60 mL of ethyl acetate was added to the reaction mixture and the organic phase was washed with (4  $\times$  20 mL) of HCl (2 M). After that, the organic phase was washed with (3  $\times$  20 mL) of NaHCO3 (0.4 M). Then, the organic solvent was dried with sodium sulfate and evaporated by a rotary evaporator. Finally, the crude product was recrystallized in hexanes to obtain the pure product as a lightyellow solid in 77 % yield (390 mg). The product was characterized by FTIR,  $^1{\rm H}$  NMR, and  $^{13}{\rm C}$  NMR (Figures S4- S6). The purity and the exact mass were shown by LC-MS (Figure S7).

### 2.5. Synthesis of curcumin dibutanoate

To a round bottom flask with a magnetic stir bar, septa, and nitrogen inlet, 300 mg (0.815 mmol) of curcumin, 0.82 mL (5.0 mmol) of butyric anhydride, 25 mg (0.20 mmol) of 4-dimethylamino pyridine, and 8 mL of acetonitrile were added. The reaction mixture was stirred at room temperature overnight under a nitrogen blanket. The progress of the reaction was followed by thin-layer chromatography (TLC). After completing the reaction, 40 mL of ethyl acetate was added to the

reaction mixture and the organic phase was washed with (4  $\times$  20 mL) of HCl (2 M). After that, the organic phase was washed with (3  $\times$  20 mL) of NaHCO<sub>3</sub> (0.4 M). Then, the organic solvent was dried with sodium sulfate and evaporated by a rotary evaporator. Finally, the crude product was recrystallized in hexanes to obtain the pure product as a yellow solid in 65 % yield (270 mg). Melting point was 132–134 °C. The product was characterized by FTIR,  $^1$ H NMR, and  $^{13}$ C NMR (Fig. 1a-1d). The purity and the exact mass were shown by LC-MS (Figure S8).

### 2.6. Synthesis of Fe(CUDB)<sub>2</sub>

27~mg of  $FeSO_4\cdot 7H_2O$  (0.1 mmol) was dissolved in 2 mL of degassed deionized water containing 2 drops of  $H_2SO_4$  (0.5 N). Then, this solution was gradually added to a stirring solution of curcumin dibutanoate (100 mg, 0.2 mmol) in a mixture of acetonitrile (9 mL) and methanol (7 mL) as a solvent. The reaction was carried out at room temperature under a nitrogen atmosphere and after 15 min, the pH of the reaction increased to around 6 by dropwise adding an aqueous solution of NaOH (0.5 N). The precipitated product was separated by centrifuge and washed with hexanes, methanol (50 %), and DI water respectively. Then, the resulting solid was freeze-dried overnight and kept in a vacuum oven at room temperature. The product was obtained as a black powder in 63.8 % yield (68.3 mg). The product was characterized by FTIR,  $^1\text{H}$  NMR, and  $^{13}\text{C}$  NMR (Figures S9-S10). The purity and the exact mass were shown by LC-MS (Fig. 3).

### 2.7. Preparation of oil solutions of curcumin and its ester derivatives

To a round bottom flask with a magnetic stir bar, 20 mg of curcumin or ester derivative was added to the corresponding oil (Table S1). After that, the flask was placed in a water bath at between 45 and 50  $^{\circ}\text{C}$  and the mixture was stirred until each sample was completely dissolved in each oil. For curcumin, curcumin diacetate, and curcumin dioctanoate sonication and heating were required to achieve clear solutions. Once the solid was dissolved, the samples were cooled to room temperature and used for the next studies. The curcumin samples were centrifuged to remove the undissolved residue and the supernatants were collected. Once dissolved, all samples remained clear during storage.

## 2.8. Preparation of Fe(CUDB)<sub>2</sub> solution in canola oil

To a culture tube containing 5.1 mg of  $Fe(CUDB)_2$ , 5 mL of canola oil was added. The mixture was vortexed for 15 min at room temperature. The concentration of this sample in canola oil was around 1.02 mg/mL.

# 2.9. Preparation of in situ $Fe(CUDB)_2$ complex in canola oil by using ethanol as a cosolvent

To a round bottom flask with a magnetic stir bar, 40 mg of curcumin dibutanoate (0.080 mmol) and 14.6 mL of canola oil were added. The flask was placed in a water bath at  $\sim$  45–50  $^{\circ}\text{C}$  and the mixture was stirred until the CUDB dissolved. Then, the sample was cooled to room temperature and 11 mg (0.080 mmol) of FeSO<sub>4</sub>·7H<sub>2</sub>O suspended in 0.4 mL of ethanol was gradually added to the oil solution and stirred for 2 h at room temperature. The color of the sample was dark red, and the concentration of the Fe(CUDB)<sub>2</sub> complex was 2.8 mg/mL.

# 2.10. Measurement of antioxidant activity of curcumin, curcumin dibutanoate, and Fe(CUDB)<sub>2</sub> by radical scavenging assay

A stock solution of each compound (1000 mg/L) was prepared in a mixture of methanol and acetonitrile (1:3), ascorbic acid and FeSO4:7H<sub>2</sub>O were dissolved in methanol at a concentration of 1000 mg/L and a 40 mg/L stock solution of 2,2-diphenyl-1-picrylhydrazyl (DPPH) was prepared by dissolving 4 mg of DPPH in 100 mL of methanol. The antioxidant activity was determined by adding 50  $\mu$ L of each compound

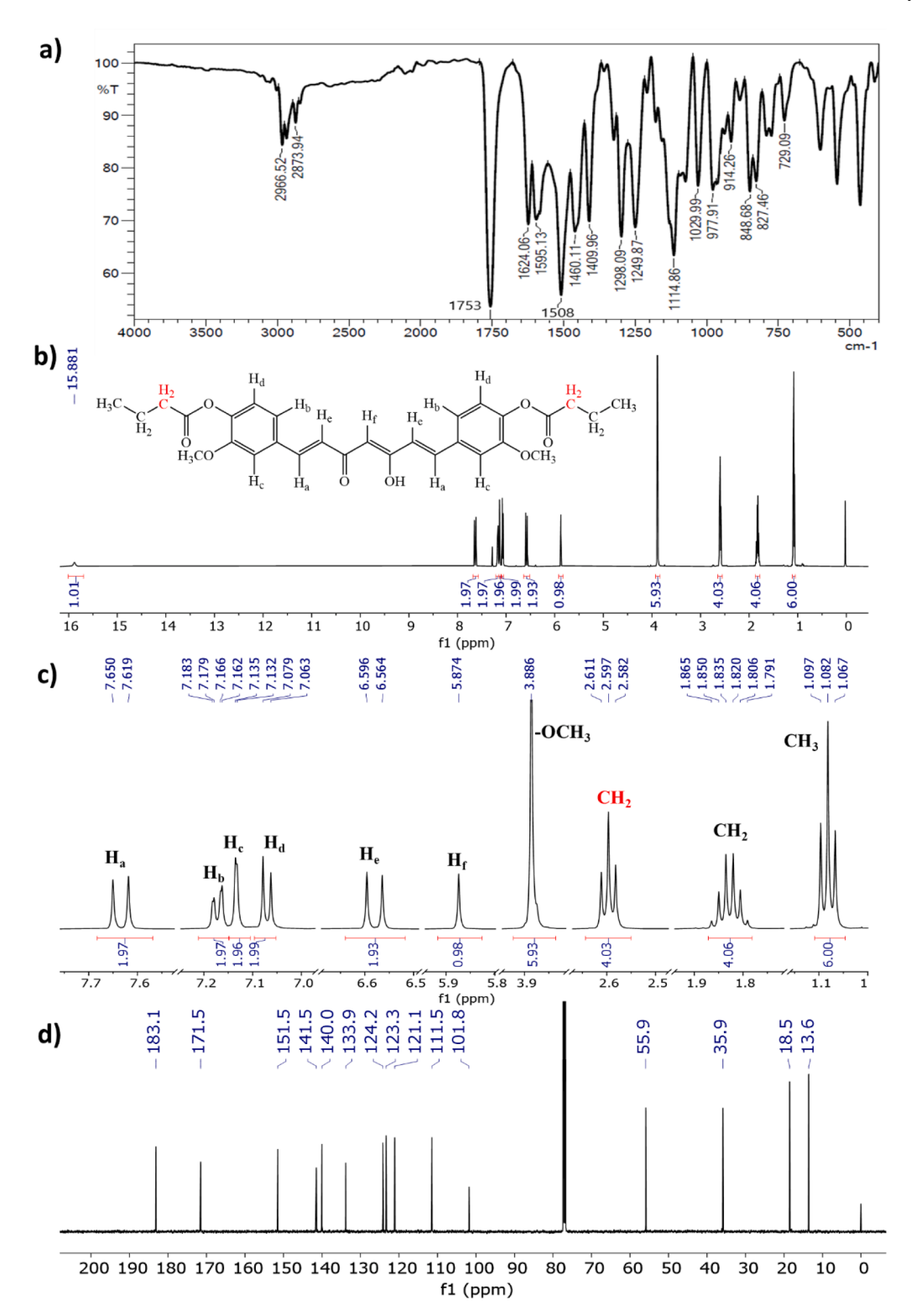


Fig. 1. a) FTIR of curcumin dibutanoate. b) <sup>1</sup>H NMR (500 MHz) of curcumin dibutanoate in CDCl<sub>3</sub>. c) Expanded <sup>1</sup>H NMR of curcumin dibutanoate in CDCl<sub>3</sub>. d) <sup>13</sup>C NMR (125 MHz) of curcumin dibutanoate in CDCl<sub>3</sub>.

solution to 5 mL of DPPH stock solution and incubating each sample in the dark for 30 min at room temperature. The absorbance of each sample was collected at 517 nm by UV–vis using DPPH sample as a blank. The percentage of the radical scavenging was calculated according to the following formula:

$$Antioxidant activity percentage = \frac{A - B}{A} \times 100 \tag{1}$$

where  $\boldsymbol{A}$  is the absorption of the blank and  $\boldsymbol{B}$  is the absorption of the sample.

# $2.11.\,$ Digestion analysis of pure curcumin dibutanoate in the simulated intestinal fluid

The simulated intestinal phase buffer was prepared by using KCl,

NaCl, KH<sub>2</sub>PO<sub>4</sub>, NaHCO<sub>3</sub>, MgCl<sub>2</sub>(H<sub>2</sub>O)<sub>6</sub>, and HCl at pH 7 according to the *Nature* protocol (Brodkorb et al., 2019). Then, in a 50 mL falcon tube, 21 mg (0.04 mmol) of curcumin dibutanoate was dissolved in 0.75 mL of DMSO. In another 50 mL falcon tube, 450 mg of porcine bile extract was dissolved in 10 mL of the buffer solution and added to the curcumin dibutanoate solution. To this solution mixture, 0.75 mL of 0.3 M CaCl<sub>2</sub> solution was added, and the pH was adjusted to  $\sim$  7 using 1 M HCl. Separately, 500 mg of fresh porcine pancreatin was dispersed in 4.5 mL of the buffer solution and then added to the curcumin dibutanoate mixture. The reaction tube was placed in an incubator at 37 °C with stirring at 250 rpm for 135 min. After that, 10 mL of 1 M HCl was added to the mixture and the released curcumin was extracted with CHCl<sub>3</sub>. The organic phase was dried with sodium sulfate and evaporated by a rotary evaporator. The remaining product was dissolved in acetonitrile and the released curcumin was measured by LC-MS.

### 3. Results and discussion

### 3.1. Synthesis of curcumin esters

We synthesized curcumin diacetate and curcumin dibutanoate as short-chain esters by the reaction of curcumin and acetic anhydride or butyric anhydride respectively. As a medium-chain ester curcumin dioctanoate was synthesized by the reaction of curcumin and *n*-octanoic anhydride.

Curcumin dibutanoate is a new compound and was characterized by FTIR,  $^1\mathrm{H}$  NMR,  $^{13}\mathrm{C}$  NMR, and LC-MS. The FTIR of curcumin dibutanoate (Fig. 1a) exhibited a broad shallow band between 3200 and 2100 cm $^{-1}$  which can be attributed to the enolic OH. The stretching vibrations of the alkene and aromatic C-Hs appear as a weak band around 3010 cm $^{-1}$ . The bands at 2966 and 2873 are ascribed to the stretching vibrations of the aliphatic C-Hs. A strong band at 1753 cm $^{-1}$  confirms the presence of the carbonyl group of the ester. A band at 1624 cm $^{-1}$  is stretching vibrations of the C=C bond. The stretching vibrations of C=C in aromatic rings appear at 1595 and 1508 cm $^{-1}$ . Two bands at 1460 and 1410 cm $^{-1}$  are the out-of-plane aliphatic C—H bending vibrations. The C—O stretching vibrations appear as the four peaks at 1298, 1249, 1114, and 1030 cm $^{-1}$ . The bands between 977 and 729 cm $^{-1}$  are attributed to the alkene and aromatic out-of-plane C—H bending vibrations.

In the <sup>1</sup>H NMR the chemical shift of enolic OH appears as a singlet peak at 15.88 ppm (Fig. 1b). Similar to curcumin, and because of the resonance between enol and ketone groups (keto-enol tautomerism), this molecule can be considered symmetric. A doublet peak ( $J_{trans}$  = 15.5 Hz) at 7.63 ppm is attributed to the two vinyl hydrogens (Ha) located at the  $\beta$  positions of the carbonyl group in the backbone of the molecule (Fig. 1c). The chemical shift of the two aromatic hydrogens (H<sub>b</sub>) is 7.17 ppm and appears as a doublet of doublets ( $J_1 = 8.5 \text{ Hz}, J_2 =$ 2 Hz). The doublet peak (J = 1.5 Hz) at 7.13 ppm is ascribed to the two aromatic hydrogens (H<sub>c</sub>) ortho to the methoxy groups on the aromatic rings. The other aromatic hydrogens (H<sub>d</sub>) appear at 7.07 ppm as a doublet peak (J = 8.0 Hz). A second doublet peak ( $J_{trans} = 16 \text{ Hz}$ ) at 6.58 ppm is attributed to the two vinyl hydrogens ( $H_e$ ) located at the  $\alpha$  position of the carbonyl group. A singlet peak at 5.87 ppm is the hydrogen of the enol group (H<sub>f</sub>) located in the center of the molecule. The presence of two methoxy groups confirms by the existence of a singlet peak at 3.89 ppm with an integral of 6. In the aliphatic ester chains, there are two CH2 groups in the vicinity of the carbonyl of ester groups that appears as a triplet peak (J = 7.5 Hz) at 2.60 ppm. The other two CH<sub>2</sub> groups are as a sextet peak (J = 7.5 Hz) at 1.83 ppm. Finally, two CH<sub>3</sub> groups appear at 1.08 ppm as a triplet peak (J = 7.5 Hz) with an integral

Like the  $^1H$  NMR, the  $^{13}C$  NMR (125 MHz) of curcumin dibutanoate was studied in CDCl $_3$  at room temperature and exhibits 15 unique carbons confirming the symmetrical structure (Fig. 1d). A peak at 183.1 ppm is attributed to the carbonyl of  $\alpha,~\beta\text{-unsaturated}$  ketone in the structure of this molecule. The carbonyl of ester groups is confirmed by

the presence of a peak at 171.5 ppm. The chemical shifts of the aromatic and vinylic carbons appear at 151.5, 141.5, 140.0, 133.9, 124.2, 123.3, 121.1, 111.5, and 101.8 ppm. A distinct peak at 55.9 ppm is attributed to the carbon two methoxy groups. In the aliphatic ester chains, the chemical shift of two  $CH_2$  groups near the carbonyl of ester groups is 35.9 ppm and the other two methylene groups appear at 18.5 ppm. In the end, the presence of a peak at around 13.6 ppm is evidence of the two  $CH_3$  groups.

In addition to NMR data, we used LC-MS to confirm purity and resolve the mass of the synthesized curcumin dibutanoate (Figure S8).

### 3.2. Oil solubility of curcumin esters

A goal of this work was to increase the oil solubility of curcumin derivatives so that they can be used in fat rich food applications. Therefore, we assessed their solubility and stability in in coconut and canola oil at room temperature (Table S1). The esterified curcumin derivatives displayed increased hydrophobicity and were subsequently more soluble in the oils. In all cases, the oil solubility in coconut oil was better than in canola oil which we attribute this to the difference in the length of triglyceride chains; canola oil has long-chain triglycerides while coconut oil is primarily composed of medium-length triglycerides (Marina et al., 2009). Among these compounds, curcumin dibutanoate had the best solubility in both coconut and canola oil. In coconut oil, its maximum solubility was 6.7 mg/mL while in canola oil its maximum solubility was 4.0 mg/mL. Further, curcumin dibutanoate is easily dissolved in organic solvents like acetone, DMSO, ethyl acetate, acetonitrile, chloroform, and methylene chloride at room temperature.

After dissolving curcumin and its ester derivatives in the oil phase, the optical properties of these compounds were studied by ultraviolet–visible (UV–vis) spectroscopy in coconut oil (Figure S11). The  $\lambda_{max}$  of curcumin diacetate, curcumin dibutanoate, and curcumin dioctanoate in coconut oil was observed at 404 nm compared to the dissolved curcumin in coconut oil that exhibited a  $\lambda_{max}$  at 423 nm. This hypsochromic shift of the esterified curcumin derivatives indicates a decrease in the resonance between the lone pair of electrons on the phenolic hydroxyl groups and the aromatic rings and thus a decrease of the  $\pi$ -delocalization is observed.

## 3.3. Thermal stability of curcumin dibutanoate

The solubility of curcumin dibutanoate in canola oil was found to be 6.7 mg/mL and in coconut oil it was 4.0 mg/mL. In each case curcumin dibutanoate showed solubility that was three to six times greater than curcumin dioctanoate and more than an order of magnitude better than curcumin or curcumin diacetate, therefore, we used curcumin dibutanoate in our stability studies (Table S1). We used  $^{1}\mathrm{H}$  NMR in DMSO- $d_{6}$  to visualize the difference in thermal stability between curcumin dibutanoate and curcumin (Fig. 2). First, curcumin (35 mg) was dissolved in DMSO- $d_{6}$  (0.9 mL) and heated at  $\sim$ 150 °C for 1 h under air atmosphere. The  $^{1}\mathrm{H}$  NMR of heated curcumin indicates that it is thermally unstable, the expanded view of the spectra contains many new peaks highlighted in red (Fig. 2a-d). This is consistent with literature reports indicating that curcumin is susceptible to oxidation and autoxidation of the phenolic hydroxyl groups during heat processing (Luis et al., 2018; Priyadarsini et al., 2003; Salem et al., 2014).

Curcumin dibutanoate was subjected to the same conditions and no differences between the <sup>1</sup>H NMR of the heated curcumin dibutanoate sample and its corresponding unheated sample were observed (Fig. 2e-h). To probe the thermal stability further, we increased the temperature to 170 °C for 1 h, and based on the <sup>1</sup>H NMR, approximately 8 % of the curcumin dibutanoate was hydrolyzed (Figures S12-S14). Curcumin dibutanoate showed remarkable heat stability that would allow the storage of this compound for months at room temperature without degradation. This is in contrast with pure curcumin which must be stored at 0 °C to maintain quality (Luis et al., 2018; Salem et al., 2014).

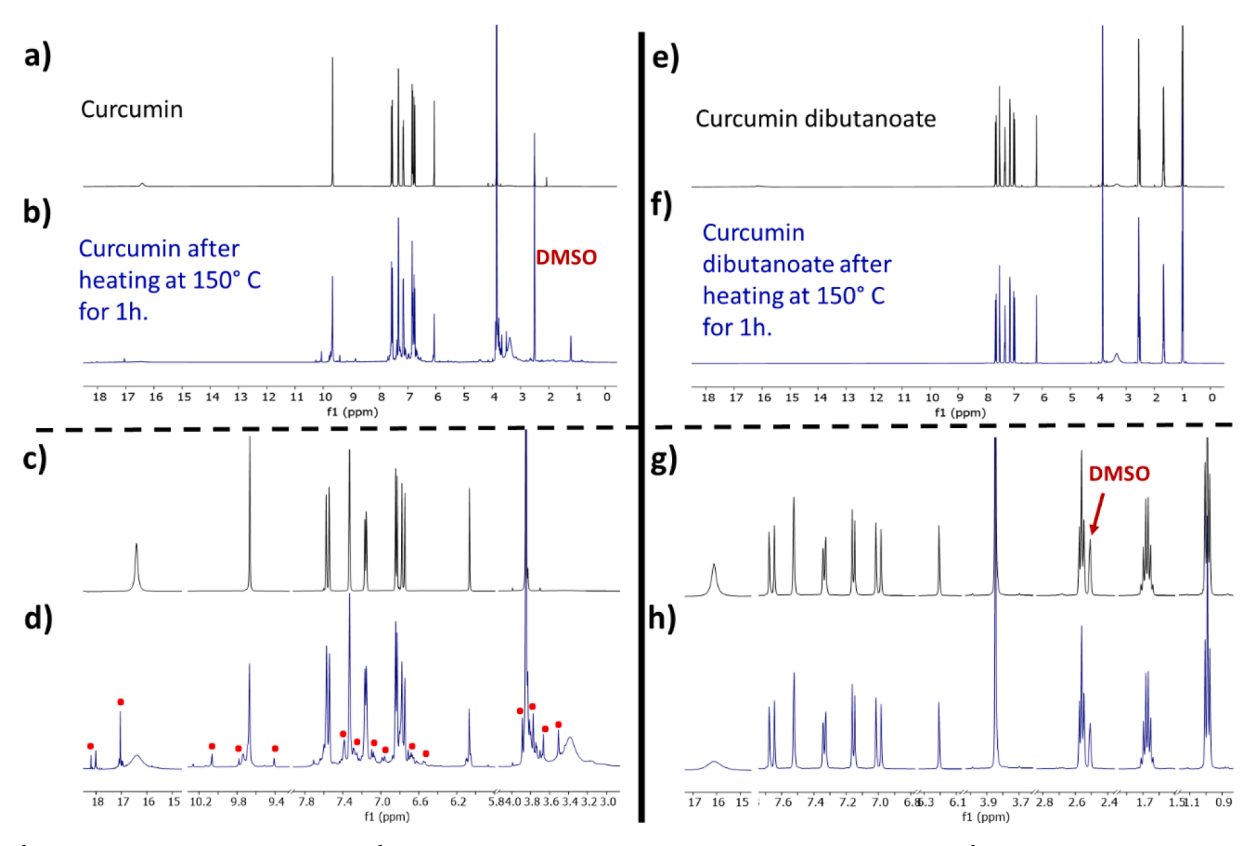


**Fig. 2.** a)  $^{1}$ H NMR of pure curcumin in DMSO- $d_{6}$ . b)  $^{1}$ H NMR of curcumin in DMSO- $d_{6}$  after heating at 150  $^{\circ}$ C. c) Expanded  $^{1}$ H NMR of pure curcumin in DMSO- $d_{6}$ . d) Expanded  $^{1}$ H NMR of curcumin in DMSO- $d_{6}$  after heating at 150  $^{\circ}$ C. e)  $^{1}$ H NMR of pure curcumin dibutanoate in DMSO- $d_{6}$ . f)  $^{1}$ H NMR of curcumin dibutanoate in DMSO- $d_{6}$  after heating at 150  $^{\circ}$ C. g) Expanded  $^{1}$ H NMR of pure curcumin dibutanoate in DMSO- $d_{6}$ . h) Expanded  $^{1}$ H NMR of curcumin dibutanoate in DMSO- $d_{6}$  after heating at 150  $^{\circ}$ C.

## 3.4. Digestibility of curcumin dibutanoate

The digestibility of curcumin dibutanoate was assessed using simulated intestinal fluid (Scheme S1). We used porcine pancreatin and a buffer solution at pH 7 according to a published Nature protocol (Brodkorb et al., 2019). Because curcumin dibutanoate is not water soluble, we used DMSO (4.4 w/w % of the total digested sample) to disperse this compound in the aqueous phase. After digestion, the quantity of curcumin released was measured by LC-MS (Figure S15). The results of the LC-MS analysis indicated that  $\sim 91$  % of the curcumin dibutanoate was hydrolyzed to curcumin and butyric acid after being exposed to the simulated intestinal fluid for 135 min. These in vitro results confirm that curcumin dibutanoate can be broken down by simulated intestinal fluid implying digestibility. Additionally, butyric acid is an important energy source for intestinal epithelial cells and gut microbiota which keep the gastrointestinal tract intact and healthy (Kolba et al., 2022b). Therefore, as a new, digestible molecule, curcumin dibutanoate has health benefits that may surpass those of natural curcumin.

# 3.5. Synthesis and characterization of Fe(CUDB)<sub>2</sub>

Curcumin readily makes metal–curcumin complexes due to the existence of an  $\alpha,\beta$ -unsaturated  $\beta$ -diketone functional group in its structure which can act as a bidentate ligand (Bicer et al., 2018; Prasad et al., 2021; Rainey et al., 2019). The most reported iron-curcumin complexes are synthesized with Fe<sup>3+</sup> because the corresponding complexes made by this cation are more stable than Fe<sup>2+</sup> (Ahmed et al., 2020; Bicer et al., 2018). There are a few reports about the in situ synthesis and use of iron (II)-curcumin complex in cell studies, but these complexes are not fully characterized (Rainey et al., 2019). Because the  $\alpha,\beta$ -unsaturated

β-diketone functional group was intact after the synthesis of curcumin dibutanoate, we used this molecule as a chelator for the synthesis of a new complex containing curcumin dibutanoate and  $Fe^{2+}$ . We used  $FeSO_4 \cdot 7H_2O$  as the source of  $Fe^{2+}$  and followed typical synthetic procedures used for the production of  $Fe(acac)_2$  (Buckingham et al., 1967). The purity and the molecular mass of the  $Fe(CUDB)_2$  complex was obtained by LC-MS and TLC (Fig. 3). The existence of a strong molecular ion peak with 1070.41 m/z confirms the presence of one  $Fe^{2+}$  and two curcumin dibutanoate ligands to produce  $Fe(CUDB)_2$  complex with  $C_{58}H_{62}FeO_{16}$  formula (Fig. 3c).

The absence in the FTIR of a broad band between 3200 and 2100 cm $^{-1}$  attributed to the enolic OH in curcumin dibutanoate confirmed the formation of the complex (**Figure S9**). The other functional groups in the curcumin dibutanoate ligand remained as expected and confirmed that the curcumin dibutanoate ligand had not degraded during complexation. The  $^{1}$ H NMR and  $^{13}$ C NMR spectra in CDCl $_{3}$  showed paramagnetic shifts which confirmed the complexation of iron and its + 2 oxidation state (**Figure S10**). The  $^{1}$ H NMR of the complex showed broad peaks for each corresponding signal due to the paramagnetic effect of iron in these structures (Amani et al., 2007; Kästele et al., 2014; Xue et al., 2011).

The oxidation state of iron in Fe(CUDB) $_2$  was confirmed using X-ray photoelectron spectroscopy (XPS). The corresponding binding energies for Fe  $2p_{1/2}$  and Fe  $2p_{3/2}$  were determined for this complex were found at 711.8 and 725.1 eV respectively which agrees with the reported XPS of the materials and complexes containing Fe $^{2+}$  (Fig. 4a) (Huang et al., 2016; Lin et al., 2018). A shoulder near the Fe  $2p_{3/2}$ , a satellite peak, at  $\sim 15.2$  eV is additional evidence of an Fe $^{2+}$  center (Huang et al., 2016; Lin et al., 2018).

Thermogravimetric analysis (TGA) of Fe(CUDB) $_2$  was measured and compared to curcumin dibutanoate to understand the role of Fe $^{2+}$  on the thermal stability of curcumin dibutanoate (Fig. 4b). The obtained results

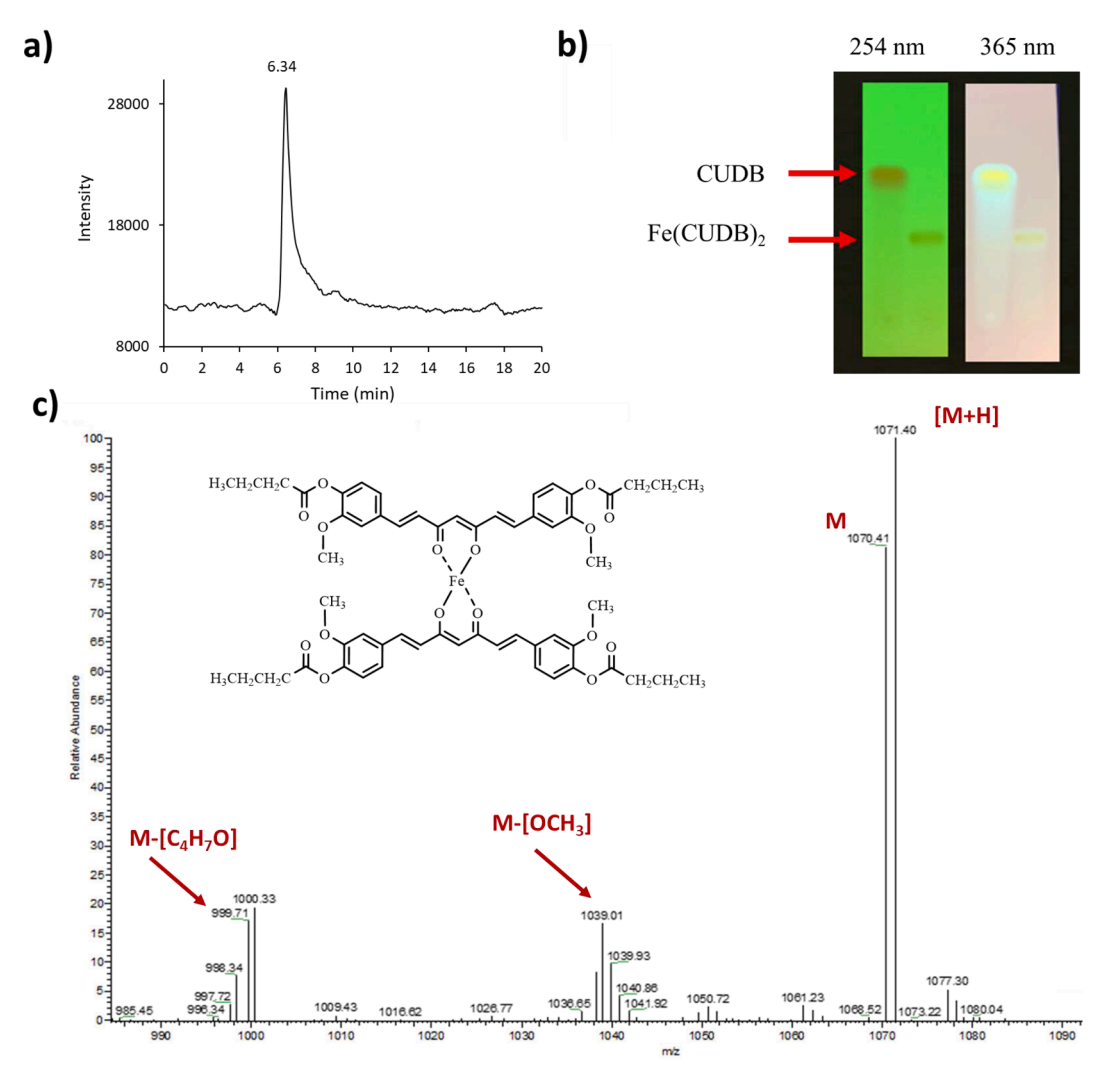


Fig. 3. a) LC of Fe(CUDB)2. (Baseline correction carried using system software.) b) TLC of Fe(CUDB)2. c) Mass spectrum of Fe(CUDB)2.

showed that by coordination of curcumin dibutanoate with  ${\rm Fe^{2+}}$  the thermal stability improved such that the  ${\rm Fe(CUDB)_2}$  complex began at to degrade at 260 °C, whereas for curcumin dibutanoate the onset of degradation was 212 °C. No ash for curcumin dibutanoate was detected at  $\sim 800$  °C, but the about 17% of the  ${\rm Fe(CUDB)_2}$  remained at 900 °C.

The crystalline structure and morphology of  $Fe(CUDB)_2$  were analyzed by powder X-ray diffraction (PXRD) and scanning electron microscope (SEM) (Fig. 4c-e). The PXRD analysis shows an intensive and sharp diffraction peak at  $4.7^{\circ}$  confirming purity and crystallinity of Fe (CUDB) $_2$  complex (Fig. 4c). This spectrum is quite different than the multiple peak spectrum that has been reported for  $FeSO_4$ ·7H $_2O$  (Huang et al., 2016). The SEM images revealed a similar morphology as accumulated crystalline shapes (Fig. 4d, e).

### 3.6. Oil solubility and thermal and oxidative stability of Fe(CUDB)2

Iron (II) is easily oxidized by moisture and air; therefore, to prevent oxidation, the oil solubility of Fe(CUDB) $_2$  was studied. Although the solubility of curcumin dibutanoate was higher in coconut oil (6.7 mg/mL) than in canola oil (4.0 mg/mL), the solubility of Fe(CUDB) $_2$  complex was higher in canola oil (1.02 mg/mL) than that of coconut oil (0.75 mg/mL). Dissolving Fe(CUDB) $_2$  in canola oil results in a clear orange-brown solution (Figures S16). UV–vis spectroscopy of the complex solution was compared to dissolved curcumin dibutanoate in canola oil (Figure S17). The  $\lambda_{max}$  of curcumin dibutanoate (404 nm) and Fe(CUDB) $_2$  (409 nm) shows the  $\pi-\pi^*$  transitions of the ligand.

Compared to curcumin dibutanoate, the existence of a broad red-shifted (bathochromic) absorption peak at around 480 nm and two weak peaks at 562 and 612 nm the confirms the charge transfer between  $Fe^{2+}$  and curcumin dibutanoate and d-d metal transitions, respectively (Ahmed et al., 2020; Al-Qudsi & Abood, 2013; Bagchi et al., 2015; El-Sayed et al., 2022; Rainey et al., 2019). Using 2.6 w/w % ethanol as a cosolvent in canola oil, we were able to in situ coordinate the  $Fe^{2+}$  with the curcumin dibutanoate, and noticed that the solubility of the resulting complex increased to 2.8 mg/mL. The UV–vis spectrum confirmed that the complex formed was the same as the stepwise synthesized  $Fe(CUDB)_2$  (Figure \$18).

For further assurance of the nature of the iron center, the EPR of this complex was measured in canola oil (Figure S19). The value of constant radiofrequency and the external magnetic field at resonance was 9.32 GHz and 1529 Gauss (0.1529 T) respectively. Considering these parameters, the magnetic moment was measured as 2.17  $\mu_B$  which according to the literature confirms the presence of Fe $^{2+}$  in this sample (Sedoud et al., 2011).

The antioxidant activity of curcumin dibutanoate and Fe(CUDB)<sub>2</sub> was studied and compared to curcumin, ascorbic acid, and FeSO<sub>4</sub>·7H<sub>2</sub>O (Table 1). A radical scavenging assay was performed by adding 50  $\mu L$  of each compound solution (1 mg/mL) to 5 mL of a 0.004 % methanolic solution of 2,2-diphenyl-1-picrylhydrazyl (DPPH) radical (Kumar et al., 2010). Compared to curcumin, the antioxidant activity of curcumin dibutanoate was significantly lower, we attribute this to the conversion of curcumin's phenolic hydroxyl groups to the corresponding butanoate

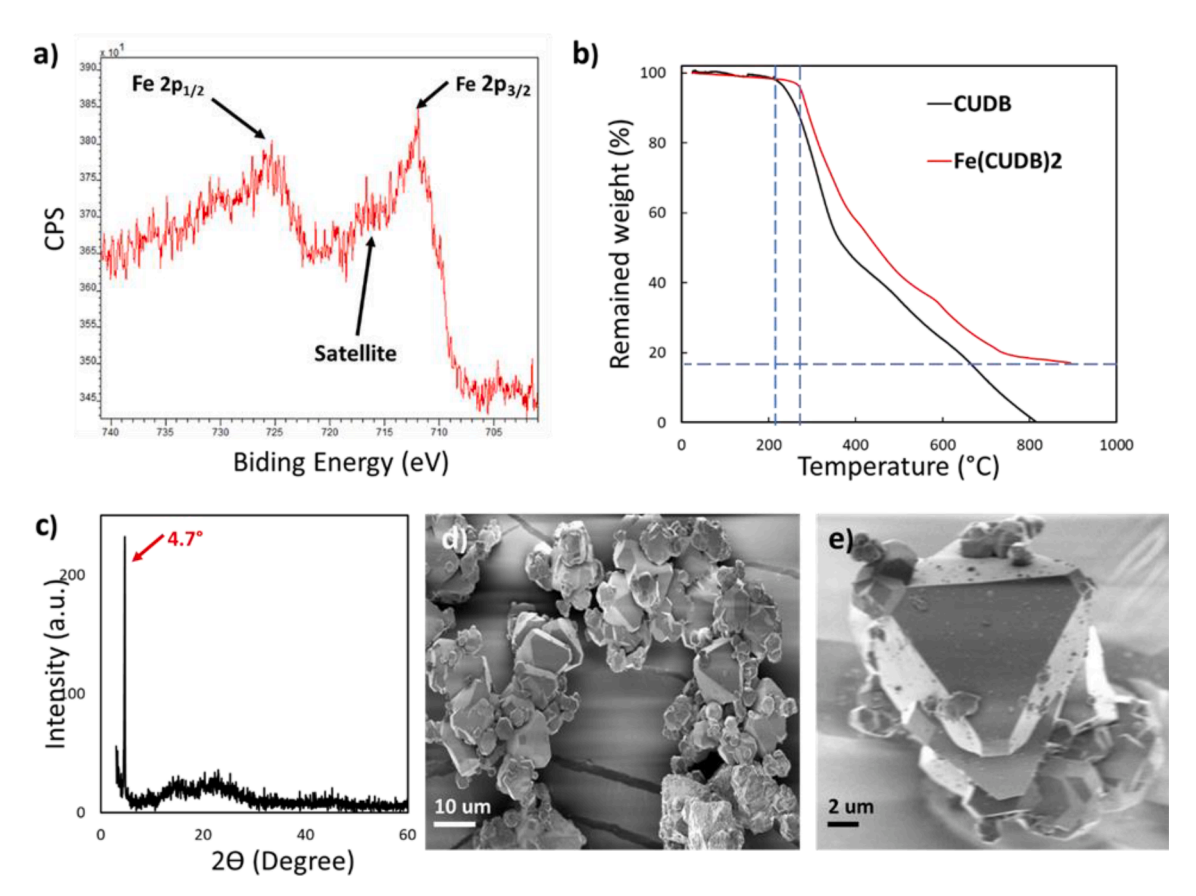


Fig. 4. a) XPS of Fe(CUDB)2. b) TGA of curcumin dibutanoate and Fe(CUDB)2. c) PXRD of Fe(CUDB)2. d) and e) SEM of Fe(CUDB)2.

**Table 1**Evaluation of the antioxidant activity of ascorbic acid, curcumin, curcumin dibutanoate, and Fe(CUDB)<sub>2</sub> using DPPH radical.

Entry	Compound	Antioxidant activity (%) <sup>a</sup>
1	ascorbic acid	$97.31 \pm 0.06$
2	curcumin	$57.79 \pm 0.11$
3	curcumin dibutanoate	$1.92\pm0.11$
4	Fe(CUDB) <sub>2</sub>	$6.79 \pm 0.08$
5	FeSO <sub>4</sub> ·7H <sub>2</sub> O	$42.73 \pm 0.06$

<sup>&</sup>lt;sup>a</sup>The measurements were performed in triplicate.

ester groups. The conversion of these groups to esters, however, is most likely why curcumin dibutanoate shows more stability than curcumin. A positive effect on the antioxidant activity was observed for  $Fe(CUDB)_2$  where antioxidant activity increased more than three times than that of curcumin dibutanoate (Table 1, entry 4).

Regarding the concentration of each compound solution (1.0 mg/ mL), the moles of curcumin dibutanoate are twice the moles of Fe<sup>2+</sup> therefore in a 50  $\mu L$  solution of the complex there are 1.0  $\times$  10<sup>-7</sup> mol of CUBD and  $5.0 \times 10^{-8}$  mol of Fe<sup>2+</sup>. This amount for Fe<sup>2+</sup> in 50  $\mu L$  of  $FeSO_4 \cdot 7H_2O$  solution is  $1.8 \times 10^{\text{--}7}$  mol. Therefore, the antioxidant activity of Fe(CUDB)<sub>2</sub> is theoretically calculated at 11.87 %. However, in the real sample, it was measured at 6.79 % (Table 1, entry 4). By coordinating Fe<sup>2+</sup> between two large and hydrophobic curcumin dibutanoate molecules the availability of the oxidant to Fe<sup>2+</sup> decreases and consequently, the antioxidant activity is roughly half the theoretically calculated activity. In sum, Fe(CUDB)2 is less easily oxidized when compared to FeSO<sub>4</sub>·7H<sub>2</sub>O or curcumin; a valuable property for the longtime storage of this complex. Further, the high digestibility of curcumin dibutanoate to curcumin not only increases its antioxidant activity by releasing curcumin in the gastrointestinal tract but also makes an improvement of iron and curcumin bioavailability (Bagchi et al.,

2015; Lorinczova et al., 2021). The main goal of this study is to improve iron oxidative stability and ensure co-delivery of iron (II) and curcumin to the GI tract with a minimum amount of oxidation. The lower antioxidant activity observed for our complexes, demonstrates the protective qualities of the two CUDB ligands against oxidation of the Fe (II) center compared to free iron. We expect that when the complex is digested the curcumin dibutanoate will undergo hydrolysis and therefore the curcumin regain its antioxidant activity. The relatively enhanced stability of the Fe(CUDB)<sub>2</sub> complex towards oxidation enables longer shelf life and higher stability of iron (II) prior to ingestion.

As a short-term storage, Fe(CUDB)<sub>2</sub> was stable in canola oil at room temperature for two months. We studied the stability of this complex in canola oil at higher temperatures (120 and 170 °C) for 30 min. The thermal stability results at 120 °C showed that no considerable change was observed after 30 min (Figure S20). Heating at 170 °C for 5 min there was no observable changes in the color, and the UV-vis spectra of the Fe(CUDB)<sub>2</sub> before and after heating in canola oil were similar. (Figure S20). However, after 15 min of heating at this temperature, upon cooling a brown sediment formed, the color intensity decreased, and a blue shift in the UV-vis was observed in the  $\lambda_{max}$  of Fe(CUDB)<sub>2</sub> from 409 nm (unheated sample) to 395 nm (Figure S20).

Further studies for measuring the bioavailability of  $Fe(CUDB)_2$  and the long-term storage stability of this complex in the oil phase and oil-inwater emulsions are in progress in our lab.

### 4. Conclusions

In summary, using acetic, butyric, and *n*-octanoic anhydrides in the presence of a catalytic amount of DMAP curcumin diacetate, curcumin dibutanoate, and curcumin dioctanoate ester derivatives were made in good to high yields. Among curcumin and its ester derivatives, curcumin dibutanoate showed the best results in terms of oil solubility in coconut

oil (6.7 mg/mL) and canola oil (4.0 mg/mL). Compared to curcumin, curcumin dibutanoate showed more stability against oxidation and heat. Curcumin dibutanoate was highly digestible in a simulated intestinal fluid and released curcumin and butyric acid as two nutritionally valuable products. Due to the high solubility of curcumin dibutanoate in the oil phase, we synthesized Fe(CUDB)2 as a new oil soluble iron (II) complex by the reaction of curcumin dibutanoate and FeSO<sub>4</sub>·7H<sub>2</sub>O. The structure and purity of these compounds were confirmed by FTIR, <sup>1</sup>HNMR, <sup>13</sup>CNMR, UV-vis, and LC-MS. The XPS and EPR results proved that the oxidation state of iron (II) was conserved during the synthesis. The results of SEM and PXRD demonstrated the crystalline structure of  $Fe(CUDB)_2$ . TGA studies verified that the thermal stability of  $Fe(CUDB)_2$ was higher than that of curcumin dibutanoate. Finally, the antioxidant activity of the present complex was studied using DPPH radical. Due to the existence of Fe<sup>2+</sup> in the structure of Fe(CUDB)<sub>2</sub>, it showed better radical scavenging activity compared to curcumin dibutanoate. The steric hindrance and the hydrophobicity of the ligand increased the stability of the Fe<sup>2+</sup> center when compared to FeSO<sub>4</sub>·7H<sub>2</sub>O. Because Fe (CUDB)<sub>2</sub> was synthesized from the functionalized natural product it can potentially be introduced as a new form of oil-soluble iron supplement which co-delivers iron (II) and curcumin.

### **Declaration of Competing Interest**

The authors declare that they have no known competing financial interests or personal relationships that could have appeared to influence the work reported in this paper.

### Data availability

Data will be made available on request.

## Acknowledgments

The authors made use of the Cornell Center for Materials Research Shared Facilities which are supported through the NSF MRSEC program (DMR-1719875). The authors also made use of the Cornell University NMR Facility, which is supported, in part, by the NSF through MRI award CHE-1531632. We also acknowledge Prof. Jack H. Freed and Liqi Lai for EPR measurements conducted at National Resource for Advanced Electron-Spin Resonance Spectroscopy (ACERT) at Cornell University which is supported by grant 1R24GM146107 from the National Institute of General Medical Sciences (NIGMS), part of the National Institutes of Health.

### Appendix A. Supplementary data

Supplementary data to this article can be found online at https://doi.org/10.1016/j.foodchem.2023.137085.

### References

- Abbaspour, N., Hurrell, R., & Kelishadi, R. (2014). Review on iron and its importance for human health. Journal of Research in Medical Sciences: The Official Journal of Isfahan University of Medical Sciences, 19(2), 164.
- Ahmed, S. A., Hasan, M. N., Bagchi, D., Altass, H. M., Morad, M., Jassas, R. S., ... Alharbi, A. (2020). Combating essential metal toxicity: Key information from optical spectroscopy. ACS Omega, 5(25), 15666–15672.
- Al-Qudsi, Z. N., & Abood, H. M. (2013). The electronic transition behavior Cr (III), Fe (III), Fe (II) and Ni (II), transition metal cations in ammonium alum-urea room temperature ionic liquid. Al-Nahrain Journal of Science, 16(3), 46–55.
- Amani, V., Safari, N., Khavasi, H. R., & Mirzaei, P. (2007). Iron (III) mixed-ligand complexes: Synthesis, characterization and crystal structure determination of iron (III) hetero-ligand complexes containing 1, 10-phenanthroline, 2, 2'-bipyridine, chloride and dimethyl sulfoxide, [Fe (phen) Cl3 (DMSO)] and [Fe (bipy) Cl3 (DMSO)]. Polyhedron, 26(17), 4908–4914.
- Assunção, M., Santos-Marques, M. J., Carvalho, F., & Andrade, J. P. (2010). Green tea averts age-dependent decline of hippocampal signaling systems related to antioxidant defenses and survival. Free Radical Biology & Medicine, 48(6), 831–838.

Bagchi, D., Chaudhuri, S., Sardar, S., Choudhury, S., Polley, N., Lemmens, P., & Pal, S. K. (2015). Modulation of stability and functionality of a phyto-antioxidant by weakly interacting metal ions: Curcumin in aqueous solution. RSC Advances, 5(124), 102516–102524.

- Basile, V., Ferrari, E., Lazzari, S., Belluti, S., Pignedoli, F., & Imbriano, C. (2009). Curcumin derivatives: Molecular basis of their anti-cancer activity. *Biochemical Pharmacology*, 78(10), 1305–1315.
- Bicer, N., Yildiz, E., Yegani, A. A., & Aksu, F. (2018). Synthesis of curcumin complexes with iron (iii) and manganese (ii), and effects of curcumin-iron (iii) on Alzheimer's disease. New Journal of Chemistry, 42(10), 8098–8104.
- Brodkorb, A., Egger, L., Alminger, M., Alvito, P., Assunção, R., Ballance, S., ... Carrière, F. (2019). INFOGEST static in vitro simulation of gastrointestinal food digestion. Nature Protocols, 14(4), 991–1014.
- Buckingham, D. A., Gorges, R. C., & Henry, J. T. (1967). The polymeric nature of Bis (acetylacetonato)-, Bis (trifluoroacetylacetonato)-, Bis (hexafluoroacetylacetonato)-, and Bis (2, 2, 6, 6-tetramethylheptane-3, 5-dionato)-iron (II). Australian Journal of Chemistry, 20(2), 281–296.
- El-Sayed, N. M. A., Elsawy, H., & Adam, M. S. S. (2022). Polar and nonpolar iron (II) complexes of isatin hydrazone derivatives as effective catalysts in oxidation reactions and their antimicrobial and anticancer activities. *Applied Organometallic Chemistry*, 36(5), e6662.
- Haas, J. D., & Brownlie, T., IV (2001). Iron deficiency and reduced work capacity: A critical review of the research to determine a causal relationship. *The Journal of Nutrition*, 131(2), 6768–6908.
- Huang, Y., Ni, H., & Rahman, S. (2016). Synthesis, characterization, and electrochemical properties of lithium-based fluorosulfate nanoparticles as cathode for lithium-ion batteries. *Ionics*, 22(10), 1775–1780.
- Jáuregui-Lobera, I. (2014). Iron deficiency and cognitive functions. Neuropsychiatric Disease and Treatment, 10, 2087.
- Jurenka, J. S. (2009). Anti-inflammatory properties of curcumin, a major constituent of Curcuma longa: A review of preclinical and clinical research. Alternative Medicine Review. 14(2).
- Kästele, X., Sturm, C., & Klüfers, P. (2014). 13C NMR spectroscopy as a tool for the in situ characterisation of iron-supplementing preparations. European Journal of Pharmaceutics and Biopharmaceutics, 86(3), 469–477.
- Kolba, N., Zarei, A., Cheng, J., Agarwal, N., Dadmohammadi, Y., Khazdooz, L., ... Tako, E. (2022a). Alterations in intestinal brush border membrane functionality and bacterial populations following intra-amniotic administration (Gallus gallus) of catechin and its derivatives. *Nutrients*, 14(19), 3924. https://doi.org/10.3390/ nu14193924
- Kolba, N., Zarei, A., Cheng, J., Agarwal, N., Dadmohammadi, Y., Khazdooz, L., ... Tako, E. (2022b). Alterations in Intestinal Brush Border Membrane Functionality and Bacterial Populations Following Intra-Amniotic Administration (Gallus gallus) of Nicotinamide Riboside and Its Derivatives. *Nutrients*, 14(15), 3130.
- Kumar, M., Sharma, K., Samarth, R. M., & Kumar, A. (2010). Synthesis and antioxidant activity of quinolinobenzothiazinones. European Journal of Medicinal Chemistry, 45 (10), 4467–4472.
- Lin, X., Chen, M., Janotti, A., & Opila, R. (2018). In situ XPS study on atomic layer etching of Fe thin film using Cl2 and acetylacetone. *Journal of Vacuum Science and Technology A*, 36(5), Article 051401.
- Liu, Z.-J., Li, Z.-H., Liu, L., Tang, W.-X., Wang, Y., Dong, M.-R., & Xiao, C. (2016). Curcumin attenuates beta-amyloid-induced neuroinflammation via activation of peroxisome proliferator-activated receptor-gamma function in a rat model of Alzheimer's disease. Frontiers in Pharmacology, 7, 261.
- Lopez, A., Cacoub, P., Macdougall, I. C., & Peyrin-Biroulet, L. (2016). Iron deficiency anaemia. *Lancet*, 387(10021), 907–916.
- Lorinczova, H. T., Begum, G., Renshaw, D., & Zariwala, M. G. (2021). Acute administration of bioavailable curcumin alongside ferrous sulphate supplements does not impair iron absorption in healthy adults in a randomised trial. *Nutrients*, 13 (7), 2300.
- Luis, P. B., Boeglin, W. E., & Schneider, C. (2018). Thiol reactivity of curcumin and its oxidation products. *Chemical Research in Toxicology*, 31(4), 269–276.
- Marina, A. M., Man, Y. C., & Amin, I. (2009). Virgin coconut oil: Emerging functional food oil. Trends in Food Science and Technology, 20(10), 481–487.
- Milman, N. T. (2020). A review of nutrients and compounds, which promote or inhibit intestinal iron absorption: Making a platform for dietary measures that can reduce iron uptake in patients with genetic haemochromatosis. *Journal of Nutrition and Metabolism*.
- Prasad, S., DuBourdieu, D., Srivastava, A., Kumar, P., & Lall, R. (2021). Metal-curcumin complexes in therapeutics: an approach to enhance pharmacological effects of curcumin. *International Journal of Molecular Sciences*, 22(13), 7094.
- Priyadarsini, K. I., Maity, D. K., Naik, G. H., Kumar, M. S., Unnikrishnan, M. K., Satav, J. G., & Mohan, H. (2003). Role of phenolic OH and methylene hydrogen on the free radical reactions and antioxidant activity of curcumin. Free Radical Biology & Medicine, 35(5), 475–484.
- Rainey, N. E., Moustapha, A., Saric, A., Nicolas, G., Sureau, F., & Petit, P. X. (2019). Iron chelation by curcumin suppresses both curcumin-induced autophagy and cell death together with iron overload neoplastic transformation. *Cell Death Discovery*, 5(1), 1–15.
- Salem, M., Rohani, S., & Gillies, E. R. (2014). Curcumin, a promising anti-cancer therapeutic: A review of its chemical properties, bioactivity and approaches to cancer cell delivery. RSC Advances, 4(21), 10815–10829.
- Schneider, C., Gordon, O. N., Edwards, R. L., & Luis, P. B. (2015). Degradation of curcumin: From mechanism to biological implications. *Journal of Agricultural and Food Chemistry*, 63(35), 7606–7614.

Sedoud, A., Cox, N., Sugiura, M., Lubitz, W., Boussac, A., & Rutherford, A. W. (2011). Semiquinone-Iron Complex of Photosystem II: EPR Signals Assigned to the Low-Field Edge of the Ground State Doublet of QA•–Fe2+ and QB•–Fe2+. Biochemistry, 50 (27), 6012–6021.

- Srivivasan, A., Menon, V. P., Periaswamy, V., & Rajasekaran, K. N. (2003). Protection of pancreatic beta-cell by the potential antioxidant bis-o-hydroxycinnamoyl methane, analogue of natural curcuminoid in experimental diabetes. *Journal of Pharmacy & Pharmaceutical Sciences*, 6(3), 327–333.
- Stohs, S. J., Chen, O., Ray, S. D., Ji, J., Bucci, L. R., & Preuss, H. G. (2020). Highly bioavailable forms of curcumin and promising avenues for curcumin-based research and application: A review. *Molecules*, 25(6), 1397.
- Tiekou Lorinczova, H., Fitzsimons, O., Mursaleen, L., Renshaw, D., Begum, G., & Zariwala, M. G. (2020). Co-administration of iron and a bioavailable curcumin supplement increases serum BDNF levels in healthy adults. *Antioxidants*, *9*(8), 645.
- Tuntipopipat, S., Zeder, C., Siriprapa, P., & Charoenkiatkul, S. (2009). Inhibitory effects of spices and herbs on iron availability. *International Journal of Food Sciences and Nutrition*, 60(sup1), 43–55.
- Wei, Q.-Y., Chen, W.-F., Zhou, B., Yang, L., & Liu, Z.-L. (2006). Inhibition of lipid peroxidation and protein oxidation in rat liver mitochondria by curcumin and its analogues. Biochimica et Biophysica Acta (BBA)-General Subjects, 1760(1), 70–77.
- Wessling-Resnick, M. (2017). Excess iron: Considerations related to development and early growth. The American Journal of Clinical Nutrition, 106(suppl\_6), 1600S–1605S.
- Xue, Z., Daran, J.-C., Champouret, Y., & Poli, R. (2011). Ligand adducts of bis (acetylacetonato) iron (II): A 1H NMR study. *Inorganic Chemistry*, 50(22), 11543–11551.
- Zarei, A., Khazdooz, L., Madarshahian, S., Enayati, M., Mosleh, I., Lin, T., ... Abbaspourrad, A. (2021). Synthesis, stability, and bioavailability of nicotinamide riboside trioleate chloride. *Nutrients*, 14(1), 113.